Journal of Photochemistry and Photobiology A: Chemistry 203 (2009) 40–49

Contents lists available at ScienceDirect

Journal of Photochemistry and Photobiology A: Chemistry

journal homepage: www.elsevier.com/locate/jphotochem

Anthracene labeled pyridine amides: A class of prototype PET sensors towards monocarboxylic acid

Kumaresh Ghosh*, Goutam Masanta, Asoke P. Chattopadhyay

Department of Chemistry, University of Kalyani, Kalyani, Nadia, Kolkata 741235, India

ARTICLE INFO

Article history:
Received 16 August 2008
Received in revised form 5 December 2008
Accepted 14 December 2008
Available online 25 December 2008

Keywords:
Molecular recognition
PET sensor
Monocarboxylic acid
Anthracene
Pyridine amide

ABSTRACT

Anthracene labeled pyridine amide receptors **1**–**3**, which can function as fluorescence switch towards monocarboxylic acids, have been designed and synthesized. The photophysical behaviors have been examined by fluorescence, UV–vis and NMR spectroscopy in the presence and absence of monocarboxylic acids of different acid strengths. While the emission of receptor **1** is decreased in the presence of monocarboxylic acids, the receptors **2**–**3**, on the contrary, show the reverse behavior under similar conditions.

1. Introduction

The past decade has witnessed an explosive growth in research involving various aspects of molecular recognition. Systems capable of sensing guest molecules or ions are considered to be quite useful in a variety of applications and there is a great deal of current interest in the development of fluorosensors for species ranging from charged to neutral in nature [1–9]. In this regard, photoinduced electron transfer (PET) is the most exploited mechanism for the design of the fluorosensors [10–12], which are essentially multicomponent systems comprising a signaling moiety (fluorophore) and a guest binding site (commonly called as receptor) [13]. These two units are usually separated by a σ-bonded spacer and the only communication between the signaling moiety and receptor module is via relatively long-range forces, the species being in their electronic ground states. In the photoexcited state, a strong long-range interaction develops in the form of an electron transfer from the guest-free receptor to the fluorophore. The guest, on binding to the receptor site modulates this thermodynamically favorable photoinduced electron transfer process and provides on-line and real-time analysis that may have a large impact in the field of chemical analysis.

Of the many guests (charged to neutral), monocarboxylic acids are of considerable interest due to their involvement in biological recognition processes [13]. A large number of drugs like antibiotics, analgesics and anti-inflammatory agents have carboxylic moiety. It is also noteworthy that in peptide recognition by vancomycin, amide-carboxylate binding is crucial [14,15]. To date, several sensors have been reported using hydrogen bonding functional groups, such as amides [16–19], ureas [7,20] and guanidiniums [21,22] to bind carboxylic acids and carboxylates. However, PET sensors for monocarboxylic acids are still rare. In the context of carboxylic acid binding, the use of pyridine amide motif is well known and has been exploited in the design of receptors for monocarboxylic acids [23,16], dicarboxylic acids [24–29], amino acids [30], etc. The attachment of such pyridine amide motif in a PET device and its hydrogen bonding-induced photophysical behavior of the PET device is unknown. We, for the first time, assembled the pyridine amide motifs with anthracene for mono [31] as well as dicarboxylic acid [32] recognition processes, respectively. In continuation of this, we report in this full account, the design, synthesis and photophysical behavior of PET-based anthryl fluorescent sensors **1**–**3** both in the presence and absence of monocarboxylic acids ranging from stronger to moderate in acid strength.

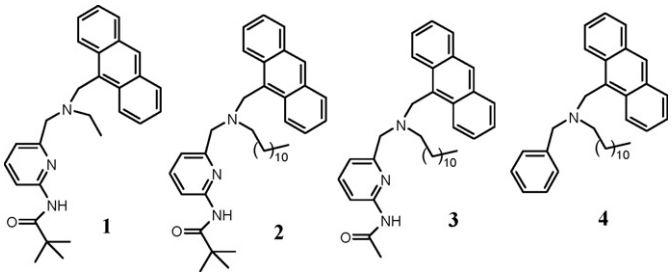

* Corresponding author. Fax: +91 33 25828282.
E-mail address: ghosh_k2003@yahoo.co.in (K. Ghosh).

1010-6030/$ – see front matter © 2008 Elsevier B.V. All rights reserved.
doi:10.1016/j.jphotochem.2008.12.017

2. Materials and methods

2.1. Materials

All the solvents were dried by usual procedures prior to use. All the reactions were carried out under nitrogen. IR and UV spectra were recorded on PerkinElmer model L120-00A and Lambda-25, respectively. Fluorescence was recorded by Spex. Fluorolog-3 (Model No. FL3-11) instrument. For ^{1}H and ^{13}C NMR spectra Bruker 200, 300, 400 and 500 MHz were used. Elemental analyses were performed on PerkinElmer 2400CHN Elemental analyzer. Melting points were recorded in open capillaries and are uncorrected.

2.2. Synthesis of **1**–**4**

2.2.1. Preparation of Schiff base (**5a**, **5b**)

To a dry MeOH solution of 9-anthraldehyde (1 mmol) at room temperature was slowly added to alkyl amine (1 mmol). After stirring at room temperature for 30 min the resulting solution was refluxed for 9 h. After cooling, the precipitated yellow solids were filtered, washed with ether. The crude yellow products were recrystallised from ethanol to yield almost pure Schiff bases (**5a**, yield 84%, m.p. 62 °C) and (**5b**, yield 77%, m.p. 56 °C). The respective Schiff bases were used for the next steps.

5a: ^{1}H NMR (400 MHz, $CDCl_3$) δ: 9.43 (s, 1H), 8.46 (d, J = 8 Hz, 3H), 8.01 (d, J = 8 Hz, 2H), 7.57–7.44 (m, 4H), 3.98 (q, J = 8 Hz, 2H), 1.52 (t, J = 4 Hz, 3H). FT-IR (KBr): 3040, 2967, 2842, 1636, and 1515 cm^{-1}.

5b: ^{1}H NMR (500 MHz, $CDCl_3$) δ: 9.41 (s, 1H), 8.47 (d, J = 10 Hz, 3H), 8.04 (d, J = 10 Hz, 2H), 7.52 (m, 4H), 3.99 (t, J = 8 Hz, 2H), 1.93 (m, 2H), 1.66–1.16 (m, 18H), 0.88 (t, J = 4 Hz 3H). ^{13}C NMR (125 MHz, $CDCl_3$): 160.0, 131.5, 130.1, 129.3, 129.1, 129.0, 126.8, 125.4, 125.1, 63.5, 32.1, 31.3, 29.9, 29.8, 29.7–29.6 (unresolved, 4 CH_2), 27.7, 22.9, and 14.4. FT-IR (KBr): 3049, 2951, 2916, 2850, 1637, and 1470 cm^{-1}.

2.2.2. N1-(6-{[(9-anthrylmethyl)(ethyl)amino]methyl}-2-pyridyl)-2,2-dimethylpropanamide (**1**)

Schiff base **5a** (0.5 g, 2.1 mmol) was dissolved in methanol (10 ml), to which a slight excess of sodium borohydride (0.12 g, 3.1 mmol) was added slowly as a solid to the methanolic solution, and the resulting solution was refluxed with stirring for 4 h. 2 M hydrochloric acid was then added to destroy the excess sodium borohydride. Once the effervescence had stopped, 2 M sodium hydroxide was added until pH 9 was obtained. The yellow solution was then extracted into chloroform, washed three times with water, separated, dried over sodium sulfate. Removal of solvent under reduced pressure afforded a crude amine **6a** (0.45 g, 89%). The crude amine **6a** (0.2 g, 0.85 mmol) without further purification and *N*1-[6-(bromomethyl)-2-pyridyl]-2,2-dimethylpropanamide (0.25 g, 0.92 mmol) were dissolved in dry acetone containing K_2CO_3 (0.5 g) and the mixture was refluxed for 5 h. The solvent was removed under reduced pressure, and the resulting mass was extracted into chloroform. After removal of the solvent the crude product was purified by column chromatography (EtOAc:Pet ether = 1:9) providing **1** (0.27 g, 75%) as a gummy product.

^{1}H NMR (200 MHz, $CDCl_3$) δ: 8.53 (d, J = 8 Hz, 2H), 8.37 (s, 1H), 7.99–7.92 (m, 4H including NH), 7.55–7.40 (m, 5H), 6.87 (d, J = 8 Hz, 1H), 4.67 (s, 2H), 3.66 (s, 2H), 2.76 (q, J = 6 Hz, 2H), 1.35–1.20 (m, 12H). ^{13}C NMR (75 MHz, $CDCl_3$): 176.9, 158.8, 150.3, 138.3, 134.0, 131.3, 130.0, 129.0, 127.5, 127.1, 125.5, 125.0, 124.7, 118.7, 111.5, 59.1, 50.4, 48.9, 27.4, and 12.0. FT-IR (KBr): 3433, 3054, 2967, 3932, 2871, 1682, and 1578 cm^{-1}. UV ($CHCl_3$): ($c = 5.05 \times 10^{-5}$ M) λ_{max} (nm) 258, 283, 350, 368, 388. MS (FAB): m/z 426 (M+1)$^+$, 396, 248, 191. Anal. Calcd. for $C_{28}H_{31}N_3O$: C, 79.02; H, 7.34; N, 9.87. Found: C, 79.08; H, 7.39; N, 9.85.

2.2.3. N1-(6-{[(9-anthrylmethyl)(dodecyl)amino]methyl}-2-pyridyl)-2,2-dimethylpropanamide (**2**)

The receptor **2** was prepared from **5b** following the same procedure as mentioned for receptor **1**. A total of 200 mg amine **6b** yielded 0.24 g of **2** (80%, gummy product) after chromatography (EtOAc:Pet ether = 1:19).

^{1}H NMR (500 MHz, $CDCl_3$) δ: 8.53 (d, J = 10 Hz, 1H), 8.37 (s, 1H), 8.01 (m, 3H), 7.88 (s, 1H), 7.59–7.39 (m, 6H), 6.99 (d, J = 10 Hz, 1H), 4.63 (s, 2H), 3.63 (s, 2H), 2.63 (t, J = 5 Hz, 2H), 1.61 (m, 2H), 1.46–1.08 (m, 27H), 0.87 (t, J = 5 Hz, 3H). ^{13}C NMR (125 MHz, $CDCl_3$): 178.0, 159.0, 150.4, 138.5, 134.8, 131.6, 129.1, 127.3 127.1, 125.6, 125.4, 124.9, 119.0, 112.0, 59.9, 55.5, 51.3, 40.9, 32.1, 29.88, 29.86, 29.82 and 29.7 (unresolved), 29.6, 27.7, 27.2, 22.9, 14.4. FT-IR (KBr): 3438, 3053, 2925, 2853, 1691, 1598, 1578, 1516, 1453 cm^{-1}. UV (CH_3CN): ($c = 5.05 \times 10^{-5}$ M) λ_{max} (nm) 286, 333, 351, 368, 388. MS (EI): m/z 565 (M$^+$), 507, 375, 208, 192, 152. Anal. Calcd. for $C_{38}H_{51}N_3O$: C, 80.66; H, 9.08; N, 7.43. Found: C, 80.63; H, 9.06; N, 7.41.

2.2.4. N1-(6-{[(9-anthrylmethyl)(dodecyl)amino]methyl}-2-pyridyl) acetamide (**3**)

The compound **2** (0.2 g, 0.35 mmol) was dissolved in 40% KOH in aqueous ethanol (15 ml) and refluxed for 15 h. The volume was reduced by evaporation of solvent and finally extracted with chloroform (20 ml × 3). The extracts were dried (Na_2SO_4) and concentrated in vacuo. The crude amine **7** was almost pure to use for the next step. The amine **7** (0.1 g, 0.21 mmol) was acetylated using acetyl chloride (0.04 ml) in the presence of triethylamine (0.04 ml) in dry CH_2Cl_2 (15 ml). After overnight stirring the solution was to afford the compound **3** (0.07 g, 66%, m.p. 74 °C). ^{1}H NMR (300 MHz, $CDCl_3$) δ: 8.50 (d, J = 9 Hz, 2H), 8.36 (s, 1H), 7.97 (d, J = 9 Hz, 2H), 7.88 (d, J = 9 Hz, 1H), 7.74 (s, 1H, –NH–), 7.52–7.42 (m, 5H), 6.93 (d, J = 9 Hz, 1H), 4.60 (s, 2H), 3.61 (s, 2H), 2.61 (t, J = 6 Hz, 2H), 2.14 (s, 3H), 1.61 (m, 4H), 1.25–1.16 (m, 16H), 0.88 (t, J = 6 Hz, 3H). FT-IR (KBr): 3267, 3053, 2924, 2853, 1696, 1599, 1578, 1538, and 1454 cm^{-1}. UV ($CHCl_3$): ($c = 5.05 \times 10^{-5}$ M) λ_{max} (nm) 283, 333, 350, 368, 388. MS (ESI): m/z 561.6 (M+K−1)$^+$, 396, 248, 191. Anal. Calcd. for $C_{35}H_{45}N_3O$: C, 80.26; H, 8.66; N, 8.02. Found: C, 80.24; H, 8.65; N, 7.99.

2.2.5. N-(9-Anthrylmethyl)-N-benzyl-N-dodecylamine (**4**)

To acetone solution (15 ml) of amine **6b** (0.2 g, 0.53 mmol) was added benzyl chloride (0.09 ml, 0.78 mmol), KI (0.13 g, 0.78 mmol) and K_2CO_3 (0.3 g) and the mixture was refluxed for 6 h under nitrogen gas. The mixture was next filtered and the solvent was removed by evaporation. The crude product was purified by chromatography (2% EtOAc in Pet ether). The compound **4** was gummy in nature and was obtained in 85% yield (0.21 g). ^{1}H NMR (200 MHz, $CDCl_3$) δ: 8.48 (d, J = 8 Hz, 2H), 8.38 (s, 1H), 8.00–7.97 (m, 2H), 7.52–7.40 (m, 4H), 7.24 (m, 5H), 4.52 (s, 2H), 3.60 (s, 2H), 2.51 (t, J = 6 Hz, 2H), 1.59 (m, 4H), 1.26 (m, 8H), 1.09 (m, 8H), 0.89 (t, J = 6 Hz, 3H). FT-IR (KBr): 3053, 3027, 2924, 2852, 1523, 1494, 1456, and 1453 cm^{-1}. UV ($CHCl_3$): ($c = 5.05 \times 10^{-5}$ M) λ_{max} (nm) 333, 350, 368, 388. Anal. Calcd. for $C_{34}H_{43}N$: C, 87.69; H, 9.31; N, 3.01. Found: C, 87.66; H, 9.28; N, 2.99.

2.2.6. General procedure of fluorescence titration

Stock solutions of the hosts were prepared in $CHCl_3$ and 1 ml of the individual host solution was taken in the cuvette. The solution was irradiated at the excitation wavelength 365 nm maintaining the excitation and emission slits 10 and 1, respectively. Upon addition of guest acids, the change in fluorescence emission of the host was noticed. The corresponding emission values during titration were noted and used for the determination of binding constant values. The change of fluorescence emission in the presence of different amounts of guest acid was used to have the Stern–Volmer plot.

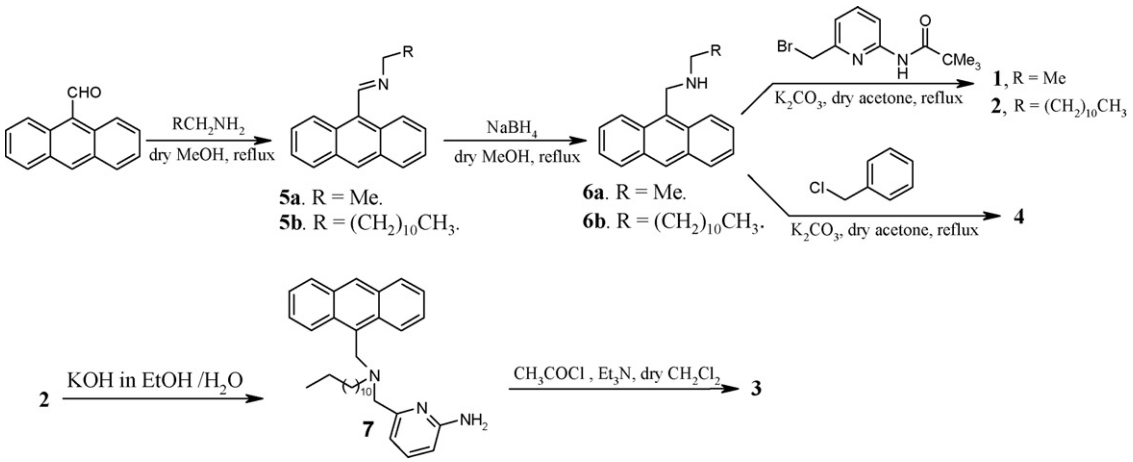

Scheme 1. Syntheses of receptors **1**, **2**, **3** and **4**.

2.2.7. General procedure of UV–vis titration

Binding constants were determined by UV–vis titration methods. Initially the receptors were dissolved in dry UV grade chloroform and taken in the cuvette. Then carboxylic acid guests, dissolved in dry $CHCl_3$, were individually added in different amounts to the receptor solution. The corresponding absorbance values during titration were noted and used for the determination of binding constant values. Binding constants were determined by using the expression $A_0/A - A_0 = [\varepsilon_M/(\varepsilon_M - \varepsilon_C)](K_a^{-1}C_g^{-1} + 1)$, where ε_M and ε_C are molar extinction coefficient for receptor and the hydrogen-bonding complex, respectively at selected wavelength, A_0 denotes the absorbance of the free receptor at the specific wavelength and C_g is the concentration of the carboxylic acid guest. The measured absorbance $A_0/A - A_0$ as a function of the inverse of the carboxylic acid guest concentration fits a linear relationship, indicating 1:1 stoichiometry of the receptor–carboxylic acid complex. The ratio of the intercept to the slope was used to determine the binding constant K_a.

3. Results and discussion

The compounds **1**–**4** were synthesized according to the Scheme 1. Their syntheses were considered via the synthesis of functionalized anthracene derivatives in introducing the pyridine amide substituent at 9-anthrylic position in order to generate the photoinduced electron transfer signal via the methylene ($-CH_2-$) bridge from the electron donor to the electron acceptor. In order to do so, anthracene labeled aliphatic amines (**6a** and **6b**) were synthesized from 9-anthraldehyde via Schiff base formation followed by reduction using sodium borohydride in dry methanol. The subsequent coupling of the amines with 2-(*N*-pivaloylamino)-6-bromomethylpyridine (obtained from bromination of 2-(*N*-pivaloylamino)-6-methyl pyridine using NBS and AIBN in dry $CHCl_3$) produced the receptors **1** and **2** in good yields. The model compound **4** was obtained in 85% yield under similar condition using benzyl chloride.

Compounds were characterized by ^{1}H NMR, ^{13}C NMR, FT-IR, mass and elemental analyses.

In all the systems **1**, **2**, **3** and **4**, anthracene, a signaling unit, has been taken into account not only due to its strong and well-characterized emission and chemical stability but also for its use by several researchers to demonstrate PET sensing. The disposition of pyridine amide (binding site) and anthracene (fluorophore) in all the sensors **1**–**3** is based on the following design principle (Fig. 1). In all designs **1**–**3** aliphatic nitrogen and pyridine amide act as *receptor 1* and *receptor 2*, respectively.

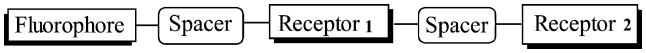

Fig. 1. Design principle of a PET sensor for carboxylic acid.

On moving from **1** to **2**, the alkyl chain around the aliphatic nitrogen center has been changed keeping the other components unchanged, to establish the role of substituent effect in sensing the carboxylic acids by anthracene labeled pyridine amide receptors. In this context, we have considered here a limited number of carboxylic acids of different acid strengths to study the photophysical behavior of **1**, **2**, **3** and **4** both in the presence and absence of acids. The receptor **3** is principally the same as **2**. Only the steric pivalamide has been replaced by acetamide for better accessibility of the amide proton in hydrogen bond formation. It is known that pyridine amide, a simple hydrogen bonding unit, forms weak two point hydrogen bond with monocarboxylic acids which are known to be present in dimeric or highly associated forms (Fig. 2).

Previously it was shown that the two-point fixation of monocarboxylic acids with 2-acetylamino-6-methylpyridine shows a binding constant of the order of 10^2 M^{-1} [33–35]. The weak binding is ascribed to the self-association of monocarboxylic acids and also the destructive hydrogen bond interactions in the hydrogen bonded complex (Fig. 2b). The dimeric state of carboxylic acid (self-association constant is of the order of 0.01–5 M^{-1}), which is resonance stabilized, is slightly converted to the monomer only at high dilution. Therefore, successful 1:1 hetero-association of carboxylic acids with receptors is only possible at the dilution of titration experiment. To investigate these weak interactions, we studied the photophysical behaviors of the systems **1**, **2**, **3** and **4** both in the presence and absence of monocarboxylic acids.

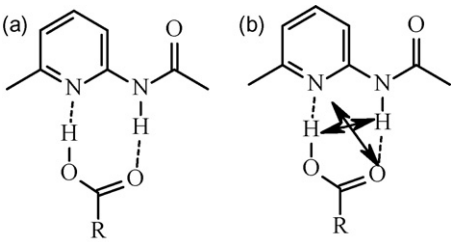

Fig. 2. (a) Two-point hydrogen bonded complex and (b) secondary hydrogen bonding interactions in the complex.

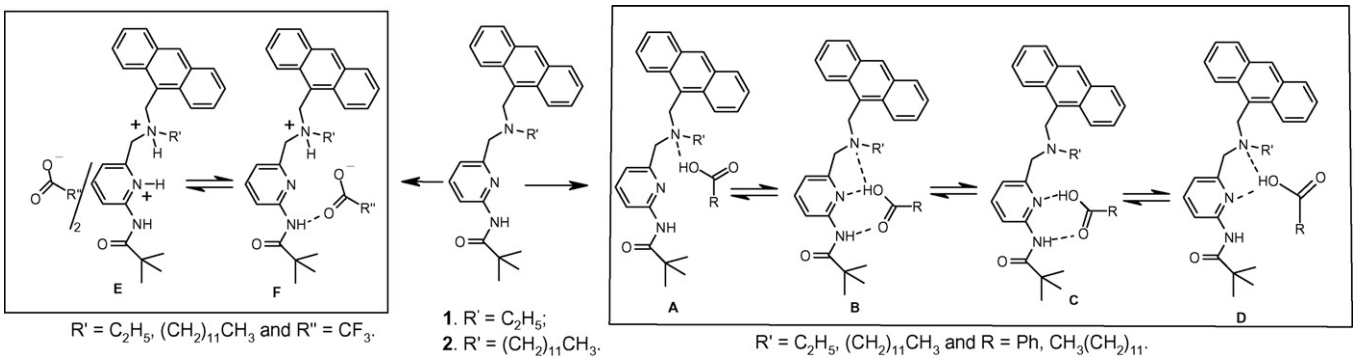

Fig. 3. Possible hydrogen bonded structures in the presence of monocarboxylic acids.

3.1. Spectroscopic studies of anthracene-based sensors ***1–4***

3.1.1. ^1H NMR study

The ^1H NMR spectra of **1** and **2** in $CDCl_3$ were recorded in the presence of monocarboxylic acids and revealed the formation of hydrogen bonded complexes by showing downfield shift of amide protons ($\Delta\delta$ = 0.10–0.50 ppm). The amide proton underwent much less downfield shift due to the steric nature of the pivaloyl group. During complexation, the more basic aliphatic nitrogen (*receptor 1*) participates in the formation of 1:1 hydrogen bonded complex as evidenced from the downfield chemical shift of all the adjacent methylene protons ($\Delta\delta$ = 0.09–0.80 ppm) along with pyridine amide (*receptor 2*) proton ($\Delta\delta$ = 0.10–0.50 ppm) in ^1H NMR. Accordingly we suggest that different possible forms of hydrogen bonded complex, of which the form **B** with benzoic and myristic acids is the more likely than the other forms **C** and **A**, may exist in solution due to greater number of hydrogen bonds (Fig. 3). The existence of form **D** where the carboxylic acid proton is simultaneously hydrogen bonded between two nitrogen atoms (from aliphatic amine and pyridine ring nitrogen), cannot be ruled out. Fig. 4, for example, demonstrates the change in chemical shift of the protons in the binding site of **1** in the presence of benzoic, myristic and trifluoroacetic acids in $CDCl_3$. During complexation the amide protons underwent weak downfield shift along with the $-CH_2-$ protons adjacent to aliphatic nitrogen. In the presence of stronger acid trifluoroacetic acid (TFA), facile protonation of both aliphatic and pyridine ring nitrogens occurs and is proved by the appearance of new peaks at 7.06 and 10.36 ppm in ^1H NMR in $CDCl_3$ for protonated ammonium and pyridinium groups, respectively [31,36]. Therefore, in case of TFA, the possible ion pairs **E** and **F** instead of pure hydrogen bonded structure **B** exist in solution. The protonated form **E** may remain in equilibrium with the form **G** where the six membered hydrogen bonding is possible. The other carboxylic acids (benzoic

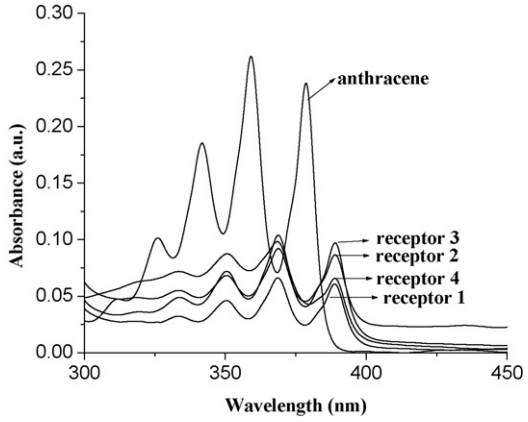

Fig. 5. UV–vis spectra of **1–4** ($c = 1.05 \times 10^{-5}$ M) in $CHCl_3$.

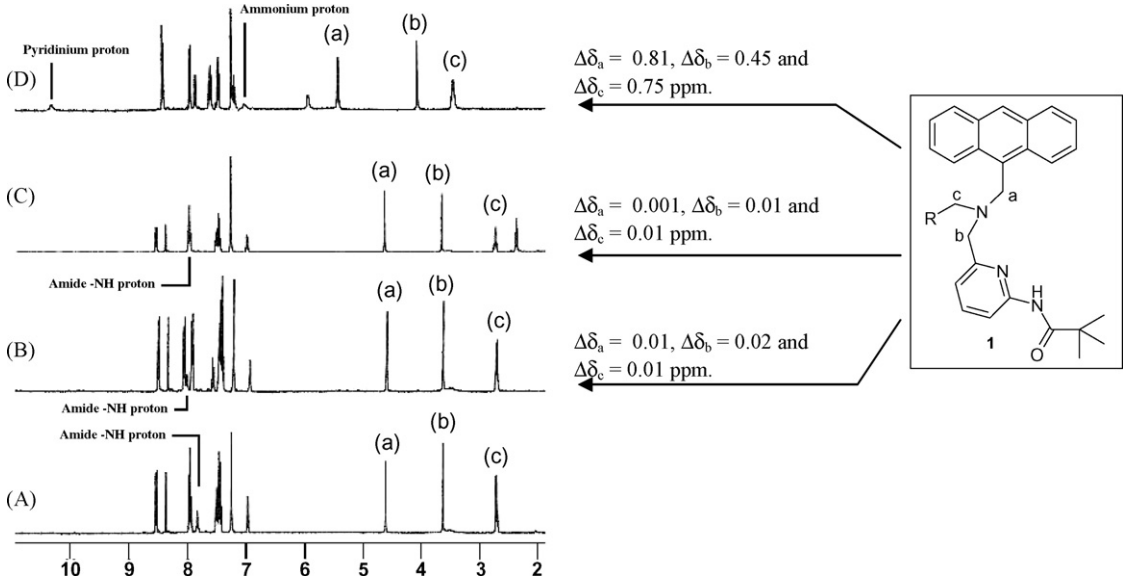

Fig. 4. Partial ^1H NMR of **1** ($c = 5.04 \times 10^{-3}$ M) in the absence of guest (A), in the presence of 1 equiv. amount of benzoic (B), myristic acids (C) and 2 equiv. amount of TFA (D).

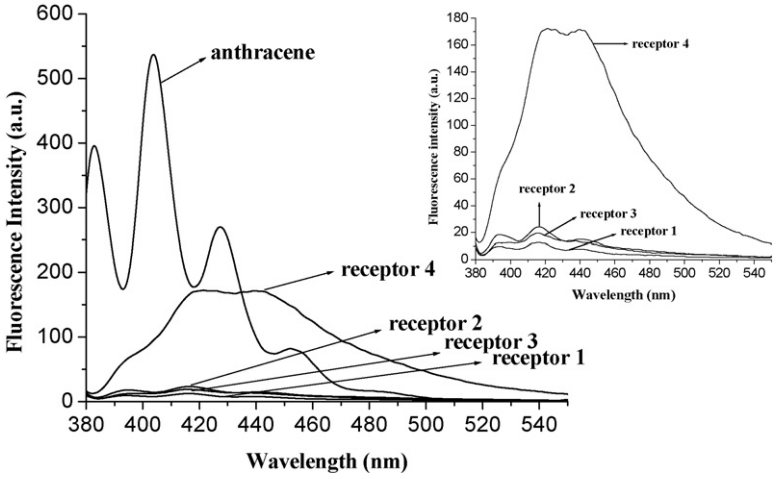

Fig. 6. Fluorescence spectra of **1**–**4** ($c = 1.05 \times 10^{-5}$ M) in $CHCl_3$ ($\lambda_{ex} = 368$ nm); inset: expanded form of emission spectra of **1**–**4**.

and myristic) studied did not exhibit such new findings under the same condition. The same was true for the receptor **2** also.

Thus these results allow us to conclude that receptors **1**–**3** form hydrogen-bonding structures with benzoic and myristic acids instead of protonation. With the ability of the pyridine amide along with the aliphatic nitrogen to form weak complexes with carboxylic acids established in ^{1}H NMR, the photophysical behavior of the receptors were examined in the presence and absence of acids.

3.1.2. *UV–vis and fluorescence studies on **1**–**4***

The ground and the excited state properties of **1**–**4** were investigated both in the presence and absence of hydrogen bond donor and acceptor solvents. The absorption spectra for all the receptors in $CHCl_3$, shown in Fig. 5, exhibit the same fine structures as is commonly observed for anthracene with red shift. For comparative purposes absorption spectra of **1**–**4** are superimposed on the absorption spectrum of anthracene in Fig. 5.

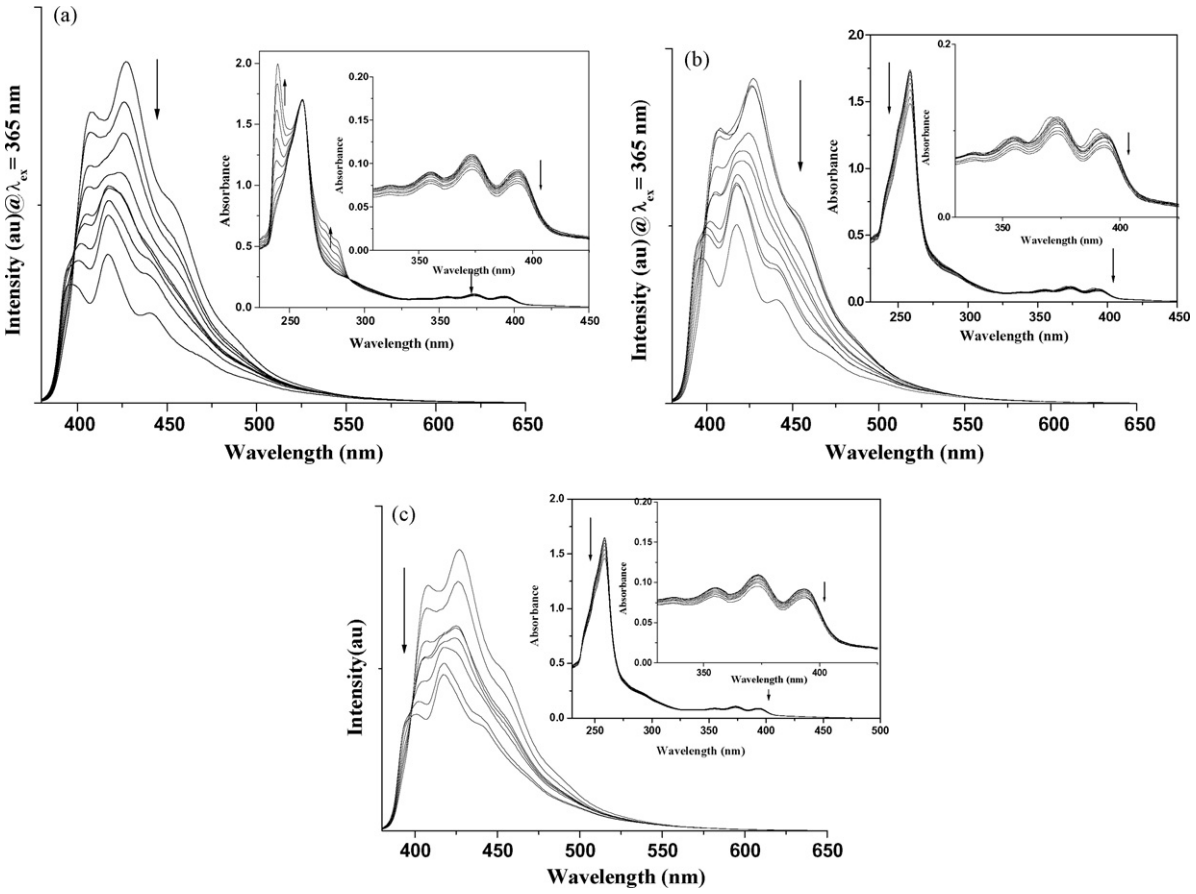

Fig. 7. (a) Fluorescence spectra of **1** ($c = 7.058 \times 10^{-5}$ M) in $CHCl_3$ upon addition of benzoic acid. Inset: change of UV–vis spectra of **1** upon addition of benzoic acid. (b) Fluorescence spectra of **1** ($c = 7.058 \times 10^{-5}$ M) in $CHCl_3$ upon addition of myristic acid. Inset: change of UV–vis spectra of **1** upon addition of myristic acid. (c) Fluorescence spectra of **1** ($c = 7.058 \times 10^{-5}$ M) in $CHCl_3$ upon addition of TFA. Inset: change of UV–vis spectra of **1** upon addition of TFA.

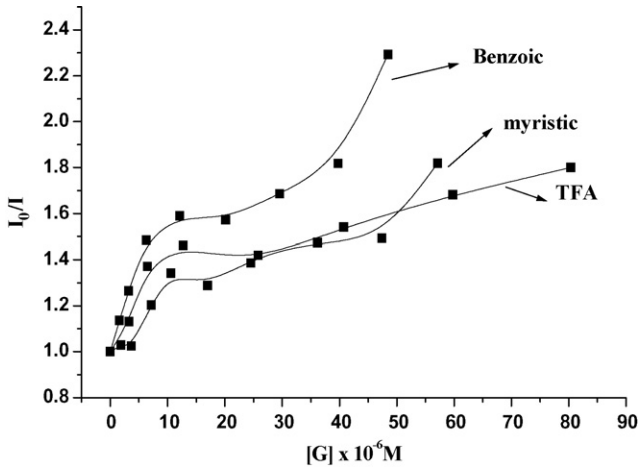

Fig. 8. Stern–Volmer plot of I_0/I vs. conc. of carboxylic acid (M).

Substituent around the aliphatic nitrogen atom in the designs **1**, **2** and **3** shows significant change in emissions (Fig. 6). In case of **4**, the quenching of the excited state of anthracene is less compared to **1**, **2** and **3**. Quantum yields are determined by the relative comparison procedure [37] using anthracene as standard (ϕ_{ant} = 0.27 in ethanol). The quantum yield values (ϕ) for **1**, **2**, **3** and **4** are found to be 0.012, 0.016, 0.012 and 0.13, respectively. This suggests that the PET is more active in **1**, **2** and **3** compared to **4**.

However, the fluorescence behaviors of **1**–**4** are quite interesting in the presence of carboxylic acids. The receptor **1** in $CHCl_3$ ($c = 7.058 \times 10^{-5}$ M) was excited at 365 nm and showed strong fluorescence intensity which gradually decreased with a little blue shift ($\Delta\lambda_{max}$ = 5–10 nm) on successive addition of benzoic (up to 50.0×10^{-6} M), myristic acid (up to 57.13×10^{-6} M) and TFA (up to 80.38×10^{-6} M) as evidenced in Fig. 7a–c, respectively, without producing any other spectral change (i.e., either exciplex or excimer formation) in the emission spectra. Slight blue shift of emission of **1** followed by quenching upon the addition of both aliphatic and aromatic monocarboxylic acids are associated with the formation of receptor–carboxylic acid complex as suggested in Fig. 2a.

Upon addition of benzoic, myristic acids and TFA the emissions were ca. 60%, 41% and 46% quenched, respectively. The Stern–Volmer plot (Fig. 8) illustrates the quenching phenomena and shows greater quenching with benzoic acid compared to myristic acid. Concurrently, the absorption spectral features of **1** in dry $CHCl_3$ ($c = 1.568 \times 10^{-5}$ M) were noted and exhibited bands centered at 393, 373 and 355 nm, attributed to anthryl moiety of **1**. The addition of monocarboxylic acids [both in case of myristic and trifluoroacetic acids (TFA)] to the solution of **1** caused a marginal decrease in intensity of the absorption peaks for anthracene (393, 373 and 355 nm) and also showed a gradual decrease in intensity of the peak centered at 258 nm shown in inset of Fig. 7b and c respectively, due to weak hydrogen bonding interactions of the pyridine amide moiety of **1** with carboxylic acid as indicated in Fig. 2a. Similarly, as shown in Fig. 7a, on gradual increase in concentration of benzoic acid, the intensity of absorption bands at 393, 373 and 355 nm were decreased gradually and exhibited a small change in intensity of the band centered at 258 nm with an isosbestic point at 290 nm along with an intensified band at 280 nm for π-stacking interaction. This observation clearly indicates the formation of 1:1 hydrogen-bonded complex. Job plots of **1** with benzoic and myristic acids also indicated the 1:1 stoichiometry in each case (Fig. 9).

In a similar way, the receptor **2** ($c = 7.079 \times 10^{-5}$ M) showed the considerable change in fluorescence when excited at 365 nm upon addition of the same carboxylic acids. The receptor **2** is almost identical with **1**, only differing in the alkyl chain attached onto the aliphatic nitrogen. The emissions of the anthryl moiety in **2**, appearing at 395, 418 and 441 nm were also similar with the receptor **1** when both were excited at 365 nm. The only interesting feature to note is that when a long dodecyl chain replaces the short ethyl chain, the switching behavior becomes reverse to that of **1**. Under similar conditions, the receptor **2** shows gradual increase in emission upon addition of carboxylic acids (Figs. 10a–c). Concurrent measurement of absorbance exhibited very little change of the absorbance of the anthryl moiety (Fig. 10a–c; insets) and indicated **2** also as an ideal PET system. The modulation of the steric nature of pivaloyl amide by less steric acetamide in **2**, leads to the receptor **3**. This also showed similar switching behavior like receptor **2** towards carboxylic acids and shows significant increase in emission in the presence of stronger acid TFA (Fig. 11). The stoichiometries of the complexes of **2** with both benzoic and myristic acids are of 1:1 like receptor **1** and were confirmed by Job plot (Fig. 12). To understand the role of pyridine amide in **1**–**3** in PET process, we took **4** as model receptor where the pyridine amide has been replaced by benzyl group. The changes in the fluorescence emission spectra of **4** in the presence of carboxylic acids were similar to that of **2** and **3**, suggesting the deactivation of PET process. This suppression of PET is due to the formation of 1:1 hydrogen-bonded complexes with benzoic and myristic acids or protonated structure with TFA (Fig. 3).

For the complexes of receptors **1**–**3**, with guests $[A_0/(A - A_0)]$ as a function of the inverse of carboxylic acid (guest) concentration fits a linear relationship, indicating 1:1 stoichiometry of receptor–carboxylic acid complex. The ratio for the intercept versus slope gives the association or binding constant (K_a) for the receptor–guest complex [38], shown in Table 1. The absorbance values at the wavelength 373 nm have been considered for determining the binding constants. Binding constant values are also determined by the similar method using fluorescence titration data.

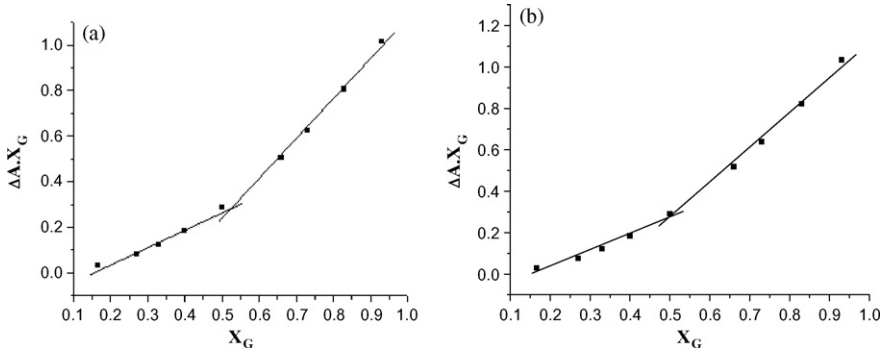

Fig. 9. Job plot of **1** with benzoic acid (a) and with myristic acid (b).

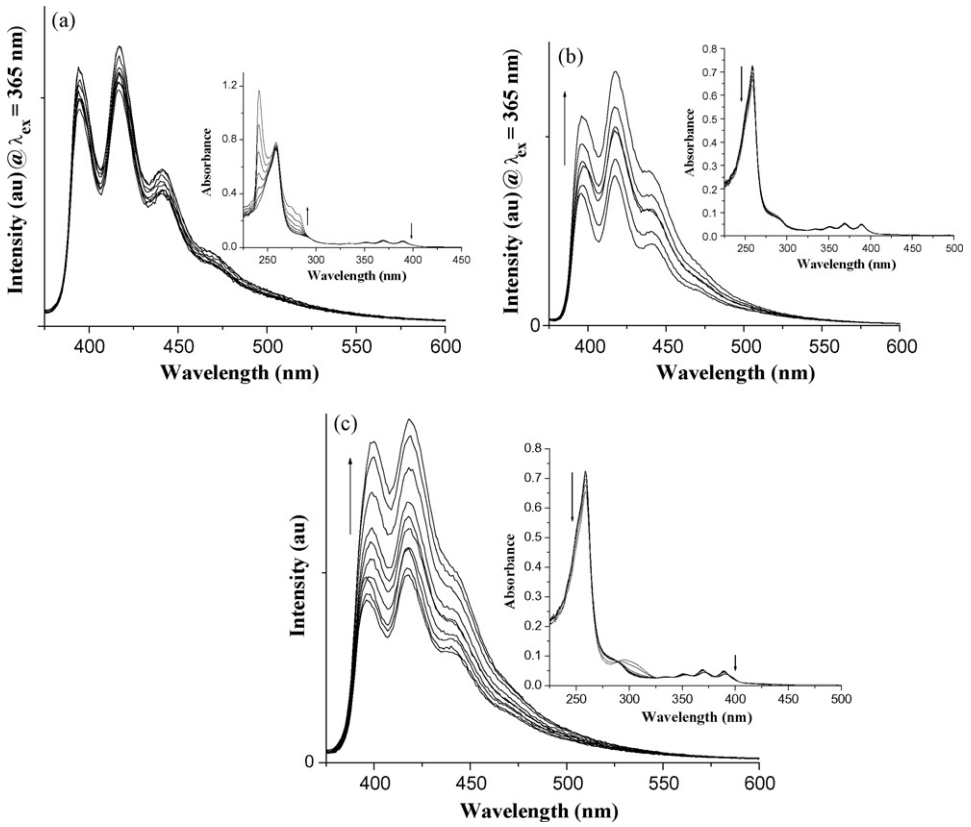

Fig. 10. (a) Fluorescence spectra of **2** ($c = 7.079 \times 10^{-5}$ M) in $CHCl_3$ upon addition of benzoic acid. Inset: change of UV–vis spectra of **2** ($c = 0.353 \times 10^{-4}$ M) upon addition of benzoic acid. (b) Fluorescence spectra of **2** ($c = 7.079 \times 10^{-5}$ M) in $CHCl_3$ upon addition of myristic acid. Inset: change of UV–vis spectra of **2** ($c = 0.353 \times 10^{-4}$ M) upon addition of myristic acid. (c) Fluorescence spectra of **2** ($c = 7.079 \times 10^{-5}$ M) in $CHCl_3$ upon addition of TFA. Inset: change of UV–vis spectra of **2** ($c = 0.353 \times 10^{-4}$ M) upon addition of TFA.

From Table 1, it appears that the receptor **1** prefers to bind benzoic than myristic acid, while for receptor **2** it is the reverse. The steric interaction between the phenyl ring of benzoic acid and the long aliphatic chain around the nitrogen center in **2** presumably reduces the binding constant value for benzoic acid than myristic acid. The increased binding constants for TFA with both **2** and **3** in the ground state indicate strong ion-pair formation compared to **1** presumably due to the presence of long carbon chain that modulates the basicity of the aliphatic nitrogen [39], although not by a large amount. This is further substantiated by our calculations of Fukui functions at the two nitrogens (viz. aliphatic, pyridine ring) for electrophilic attack on **1** and **2** [40]. In the excited state, **1** shows a higher binding with TFA compared to **2** and **3**.

3.2. Theoretical investigations on *1*–*4*

The compounds **1**–**4**, and their complexes with the monocarboxylic acids, considered in our study, were subjected to geometry optimization at AM1 [41,42] level. The optimized structures of **1** with benzoic acid, **2** and **3** with myristic acid are shown in Fig. 13.

In Table 2, some characteristic structural parameters of **1**–**4** both in the presence and absence of monocarboxylic acids have been listed.

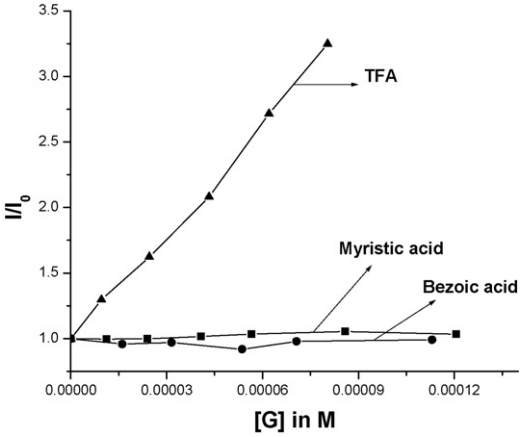

Fig. 11. Fluorescence responses of **3** ($c = 3.824 \times 10^{-5}$ M) in $CHCl_3$ upon addition of benzoic, myristic and TFA.

It is clear from the Table 2 that with increase in size of R′ (pendant substitutent on aliphatic nitrogen) anthracene and pyridine amide motifs come closer in **2** and it is significantly changed when complexation occurs with the acids. The same is true for the other

Table 1
Association constants (K_a) of **1**, **2** and **3** with guest carboxylic acids by UV and fluorescence methods.

Carboxylic acids	K_a (M^{-1}) with **1**		K_a (M^{-1}) with **2**		K_a (M^{-1}) with **3**	
	UV	Fluorescence	UV	Fluorescence	UV	Fluorescence
Benzoic	6.33×10^4	1.82×10^5	8.46×10^3	[a]	1.95×10^4	[a]
Myristic	4.96×10^3	1.72×10^3	1.32×10^4	8.33×10^4	2.61×10^4	[a]
TFA	49	3.56×10^4	4.33×10^3	6.23×10^3	6.62×10^3	4.87×10^3

[a] Binding constant values were not determined due to minor changes.

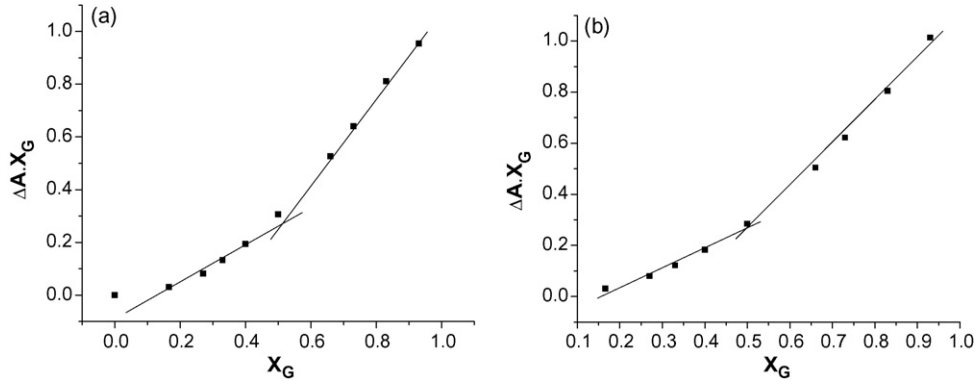

Fig. 12. Job plot of **2** with benzoic acid (a) and with myristic acid (b).

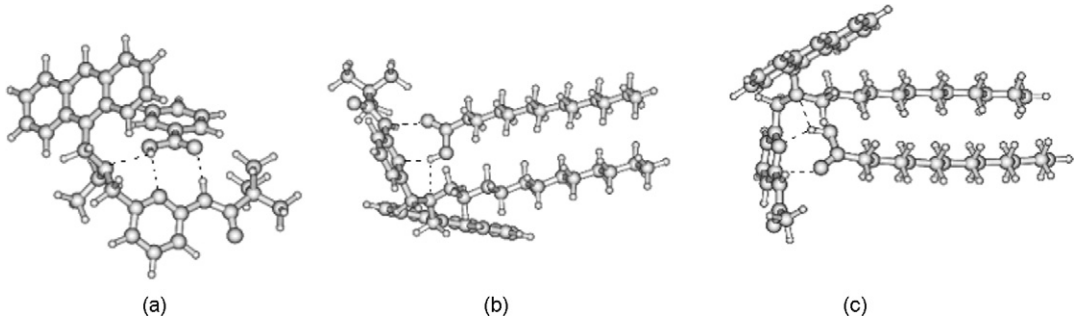

Fig. 13. AM1 optimized structures of the hydrogen-bonded complexes of receptors **1** with benzoic acid (a), **2** with myristic acid (b) and **3** with myristic acid (c).

Table 2
Distances between ring nitrogen of pyridine and anthracene (d) and the hydrogen bond lengths (r_1, r_2, r_3) as shown in Fig. 14.

Sensors	d (Å)			r_1 (Å)		r_2 (Å)		r_3 (Å)	
	Alone	BA	MA	BA	MA	BA	MA	BA	MA
1	4.837	4.643	4.621	2.130	2.135	2.673	2.669	2.755	2.758
2	4.035	3.838	4.321	4.985	2.155	2.781	2.745	2.674	2.887
3	4.848	4.429	4.424	2.248	2.176	2.533	2.728	2.892	2.923
4	–	–	–	–	–	–	–	2.708	2.867

BA = in the presence of benzoic acid, MA = in the presence of myristic acid.

compounds also. For **3**, although the size of R′ increases the distance (d) slightly for the isolated molecule, it becomes much less (though not as much as in case of **1** and **2**) when bonded with benzoic acid. Complexation of myristic acid decreases the distance for all the compounds, but much less as compared to benzoic acid. Hydrogen bond lengths are more sensitive to the size of R′ in case of **1** and **2**, for complexation with benzoic acid: r_1 and r_2 increases and r_3 decreases for these combinations. For complexation with myristic acid, r_1, r_2 and r_3 all increase, although the magnitude is much less as compared to benzoic acid.

The conclusions from the above exercise are that (i) prototype sensors **1** and **2** should be the most sensitive with respect to fluorescence behavior as the distance between the fluorophore and binding site changes and (ii) these sensors show the largest structural change when complexed with the acids. Incidentally, when compounds **2**, **3** and **4** are complexed with myristic acid, the average distance between the pendant aliphatic chain of the sensors and the aliphatic chain of the guest lie in the range of 3.9–5 Å, showing a weak chain-to-chain interaction. Also, when **4** is complexed with benzoic acid, the phenyl group of the latter is situated in between anthracene and the phenyl groups of **4**, with the average distance of 4.5 and 5.5 Å between the rings.

Thus the greatly decreased or increased fluorescence intensity of the anthracene-based sensors **1**–**3** in the presence of acid is due to the relatively stronger noncovalent interactions as well as the conformation variations in terms of distance and relative orientation between fluorophore and the receptor sites in solution which regulate PET processes in different ways. The diminished fluores-

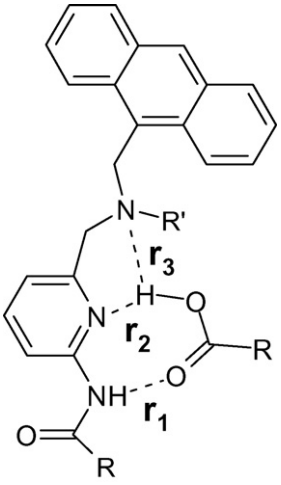

Fig. 14. Three possible hydrogen bonds in the complexes.

cence emission intensity of **1** is due to thermodynamically favored primary PET between the tertiary aliphatic nitrogen (*receptor 1*) and the excited chromophore (*Anth; *receptor 2*). Complexation of this aliphatic nitrogen will stop the primary PET and fluorescence of **1**, in principle, will be increased on the basis of normal logic of fluorescent PET sensor. But at the same time, the opposite situation, i.e., decrease in emission can be arranged by secondary PET process (*Anth to pyrdine amide). In case of **1**, there is a combination of these two opposite situations and in the more favored hydrogen bonded form **B**, the activation of secondary PET process (*Anth-to-Pyridine amide electron transfer) over the primary PET (aliphatic nitrogen to *Anth electron transfer) comes in action resulting the quenching of fluorescence. The electron deficiency of pyridine amide, either in free or complexed state, here presumably plays the significant role in activating the seceondary PET over the primary PET process reflecting the quenching of fluorescence of **1** towards monocarboxylic acids. The same is true for stronger acid TFA where there is a case of protonation of both aliphatic and pyridine ring nitrogens instead of highly hydrogen bonding structures as that of benzoic and myristic acids. In case of **2** and **3**, the presence of long aliphatic chain around the aliphatic nitrogen has marked effect on the deactivation of secondary PET process and thus exhibits a reverse switching behavior to that of **1**. Even the replacement of more steric pivaloyl amide in **2** by less steric acetamide group has a marked effect on the PET process. While **2** shows significant increase in emission in the presence of myristic acid, compound **3** exhibits little increase in the presence of the same acid. We presume that carboxylic acid motif is comfortably complexed with the pyridine amide of **3** due to less steric nature of acetamide moiety for which the aliphatic nitrogen is weakly involved in complexation and affects the PET process significantly. This is evident from the gas phase calculation in Table 2 where the hydrogen bond distance r_3 is changed and found greater in the complexes of both myristic and benzoic acids with **3**. Even the distance between anthracene and pyridine ring is also increased during complexation. This change in distance has marked effect on the both the 1^0 and 2^0-PET processes occurring in **3**.

4. Conclusions

We have presented the synthesis of a range of new functionalized anthracene labeled prototype sensors. A key aspect of the design strategy is the alteration of a substituent around the trivalent nitrogen keeping anthracene and pyridine amide fixed as fluorophore and binding site, respectively. We have established that modification of the alkyl chain residue in the anthracene labeled pyridine amide sensors alters the fluorescence behaviors towards sensing of monocarboxylic acids. All the sensors **1**, **2** and **3**, which are simple, easy to make, show good emission switchability towards carboxylic acids of different acid strengths. While the sensor **1** is more sensitive to benzoic acid, the sensor **2** is for myristic acid.

Acknowledgements

We like to thank DST and CSIR, Govt. of India, New Delhi, for financial support. G.M. is also thankful to CSIR, New Delhi, for providing fellowship. We also acknowledge DST-FIST for providing the facilities in the Department.

References

[1] K. Rurack, U. Resch-Genger, Rigidization, preorientation and electronic decoupling—the 'magic triangle' for the design of highly efficient fluorescent sensors and switches, Chem. Soc. Rev. (2002) 116–127.
[2] A.W. Czarnik, Chemical communication in water using fluorescent chemosensors, Acc. Chem. Res. 27 (1994) 302–308.
[3] S.H. Lee, H.J. Kim, Y.O. Lee, J. Vicens, J.S. Kim, Fluoride sensing with a PCT-based calix[4]arene, Tetrahedron Lett. 47 (2006) 4373–4376.
[4] C.P. Causey, W.E. Allen, Anion binding by fluorescent biimidazole diamides, J. Org. Chem. 67 (2002) 5963–59638 (references cited therein).
[5] D. Gomez, L. Fabbrizzi, M. Licchelli, Why, on interaction of urea-based receptors with fluoride, beautiful colors develop, J. Org. Chem. 70 (2005) 5717–5720.
[6] E. Fan, S.A. van Arman, S. Kincaid, A.D. Hamilton, Molecular recognition: hydrogen-bonding receptors that function in highly competitive solvents, J. Am. Chem. Soc. 115 (1993) 369–370.
[7] S.-I. Kondo, Y. Hiroka, N. Kurumatani, Y. Yano, Selective recognition of dihydrogen phosphate by receptors bearing pyridyl moieties as hydrogen bond acceptors, Chem. Commun. (2005) 1720–1722.
[8] T.W. Bell, N.M. Hext, Supramolecular optical chemosensors for organic analytes, Chem. Soc. Rev. 33 (2004) 589–598.
[9] Y. Nakahara, Y. Matsumi, W. Zhang, Kida, Toshiyuki, Y. Nakatsuji, I. Ikeda, Fluorometric sensing of alkaline earth metal cations by new lariat ethers having plural pyrenylmethyl groups on the electron-donating sidearms, Org. Lett. 4 (2002) 2641–2644.
[10] T. Gunnlaugsson, A.P. Davis, J.E. O'Brien, M. Glynn, Fluorescent sensing of pyrophosphate and bis-carboxylates with charge neutral PET chemosensors, Org. Lett. 4 (2002) 2449–2452 (references cited therein).
[11] K.-X. Xu, Y.-B. He, H.-J. Qin, G.-Y. Qing, S.-Y. Liu, Enantioselective recognition by optically active chiral fluorescence sensors bearing amino acid units, Tetrahedron Asymmetr. 16 (2005) 3042–3048.
[12] A.P. deSilva, H.Q.N. Gunaratne, T. Gunnlaugsson, A.J.M. Huxley, C.P. McCoy, J.T. Rademacher, T.E. Rice, Signaling recognitione events with fluorescent sensors and switches, Chem. Rev. 97 (1997) 1515–1566.
[13] H. Dugas, Bioorganic Chemistry, Springer, New York, 1996.
[14] E. Antonio, A. Galan, J.M. Lehn, J. Mendoza, Chiral recognition of aromatic carboxylate anions by an optically active abiotic receptor containing a rigid guanidinium binding subunit, J. Am. Chem. Soc. 111 (1989) 4994–4995.
[15] J. Fredericks, J. Yang, S.J. Geib, A.D. Hamilton, Hydrogen bonding control of molecular self-assembly, Proc. Indian Acad. Sci. (Chem. Sci.) 106 (1994) 923–935.
[16] S. Goswami, K. Ghosh, S. Dasgupta, Molecular recognition: connection and disconnection of hydrogen bonds, a case study with dimeric and highly associated monocarboxylic acids with simple receptors, Tetrahedron 52 (1996) 12223–12232.
[17] K. Ghosh, G. Masanta, Triphenylamine-based novel PET sensors in selective recognition of dicarboxylic acids, Tetrahedron Lett. 47 (2006) 2365–2369.
[18] K. Ghosh, S. Adhikari, Fluorescence sensing of tartaric acid: a case of excimer emission caused by hydrogen bond-mediated complexation, Tetrahedron Lett. 47 (2006) 3577–3581 (references cited therein).
[19] K. Choi, A.D. Hamilton, Selective anion binding by a macrocycle with convergent hydrogen bonding functionality, J. Am. Chem. Soc. 123 (2001) 2456–2457.
[20] A.I. Oliva, L. Simon, F.M. Muniz, F. Sanz, J.R. Moran, Urea–tetrahydrobenzoxanthene receptors for carboxylic acids, Tetrahedron 60 (2004) 3755–3762.
[21] B. Baragana, A.A.G. Blackburn, P. Breccia, A.P. Davis, J. deMendoza, J.M. Padron-Carrillo, P. Prados, J. Riedner, J.G. de Vries, Enantioselective transport by a steroidal guanidinium receptor, Chem. Eur. J. 8 (2002) 2931–2936.
[22] S.-I. Sasaki, A. Hashizume, D. Citterio, E. Fujii, K. Suzuki, Fluororeceptor for zwitterionic form amino acids in aqueous methanol solution, Tetrahedron Lett. 57 (2002) 7243–7245 (references cited therein).
[23] A. Bilz, T. Stork, G. Helmchen, New chiral solvating agents for carboxylic acids: discrimination of enantiotopic nuclei and binding properties, Tetrahedron Asymmetr. 8 (1997) 3999–4002.
[24] S. Goswami, K. Ghosh, S. Dasgupta, Troger's base molecular scaffolds in dicarboxylic acid recognition, J. Org. Chem. 65 (2000) 1907–1914.
[25] H. Miyaji, M. Dudic, J.H.R. Tucker, I. Prokes, M.E. Light, M.B. Hursthouse, I. Stibor, P. Lhotak, Bis(amidopyridine)-linked calix[4]arenes: a novel type of receptor for dicarboxylic acids, Tetrahedron Lett. 43 (2002) 873–878.
[26] K. Ghosh, G. Masanta, Triphenylamine-based novel PET sensors in selective recognition of dicarboxylic acids, Tetrahedron Lett. 47 (2006) 2365–2369 (references cited therein).
[27] F.G. Tellado, S. Goswami, S.K. Chang, S.J. Geib, A.D. Hamilton, Molecular recognition: a remarkably simple receptor, for the selective complexation of dicarboxylic acids, J. Am. Chem. Soc. 112 (1990) 7393–7394.
[28] C. Vincent, E. Fan, A.D. Hamilton, Molecular recognition: directed hydrogen bonding receptors for acylamino acid carboxylates, Tetrahedron Lett. 33 (1992) 4269–4272.
[29] I.L. Karle, D. Ranganathan, V. Haridas, Molecular recognition: the demonstration of 1,3-bis[(pyrid-2-ylamino)carbonyl]adamantane as an exceptionally versatile assembler of one-dimensional motifs, J. Am. Chem. Soc. 119 (1997) 2777–2783.
[30] C. Raposo, M. Martin, M.L. Mussons, M. Crego, J. Anaya, M.C. Ceballero, J.R. Moran, Chromenone derivatives as receptors for *N*-benzoylamino acids, J. Chem. Soc., Perkin Trans. (1994) 2113–2116.
[31] K. Ghosh, G. Masanta, Anthracene-appended pyridine amide: a simple sensor for monocarboxylic acids, Supramol. Chem. 17 (2005) 331–334.
[32] K. Ghosh, G. Masanta, Anthracene-coupled pyridine amines: a new "off–on" switch for molecular recognition studies on dicarboxylic acids, Chem. Lett. 35 (2006) 414–415.
[33] F. Garcia-Tellado, S. Goswami, S.K. Chang, S.J. Geib, A.D. Hamilton, J. Am. Chem. Soc. 112 (1990) 7393–7394.
[34] B. Konig, O. Moller, P. Bubenitschek, P.G. Jones, Binding of heptanedioic acid to a three fold pyridine arylamide receptor, enhancement of the stability of supramolecular solution structures by multiple binding sites, J. Org. Chem. 60 (1995) 4291–4293.

[35] M.C. Etter, D.A. Adsmond, The use of cocrystallization as a method of studying hydrogen bond preferences of 2-aminopyrimidine, J. Chem. Soc., Chem. Commun. (1990) 589–591.
[36] V. Amendola, D. Esteban-Gomiez, L. Fabbrizzi, M. Licchelli, What anions do to N–H-containing receptors, Acc. Chem. Res. 39 (2006) 343–353.
[37] Y. Wu, X. Peng, J. Fan, S. Gao, M. Tian, J. Zhao, S. Sun, Fluorescence sensing of anions based on inhibition of excited state intramolecular proton transfer, J. Org. Chem. 72 (2007) 62–70.
[38] P.T. Chou, G.R. Wu, C.Y. Wei, C.C. Cheng, C.P. Chang, F.T. Hung, Excited-state amine-imine double proton transfer in 7-azaindoline, J. Phys. Chem. B 104 (2000) 7818–7829.
[39] Y.K. Hong, W.H. Hong, Equilibrium studies on reactive extraction of succinic acid from aqueous solution with tertiary amine, Bioproc. Eng. 22 (2000) 477–481 (references cited therein. Although qualitative, the above reference clearly shows the effect of chain length on physical properties. Also, pKa values of some conjugated acids of trialkylamines are: Me_3NH^+ (9.75), Et_3NH^+ (10.67), Pr_3NH^+ (10.65), Bu_3NH^+ (9.93) [data taken from "Dissociation constants of organic bases in aqueous solution", D.D. Perrin, Butterworths, 1965, London]. These results indicate that alkyl chain length alters basicity of amines, albeit possibly in small amounts).
[40] Fukui function (f_k^-), calculated as $\rho_k(N) - \rho_k(N-1)$, where $\rho_k(N)$ is the population at the kth site for an N electron system, measures the propensity of the site for electrophilic attack. The larger the value, the more is the reactivity of the site towards an electrophile. For compound **1**, value of the function at aliphatic nitrogen is 0.00456, for compound **2** it is 0.01091. Values of the function for pyridine ring nitrogens in **1** and **2** are 0.00731 and 0.00468, respectively. Clearly, the aliphatic nitrogen of **2** is the most favored site for electrophilic attack. The calculations were done with cc-pVDZ basis and B3LYP functional at the AM1 optimized geometries of **1** and **2**;
(a) P. Geerlings, F. De Proft, W. Langenaeker, Conceptual density functional theory, Chem. Rev. 103 (2003) 1793–1874;
(b) P.K. Chattaraj, U. Sarkar, D.R. Roy, Electrophilicity index, Chem. Rev. 106 (2006) 2065–2091.
[41] M.J.S. Dewar, E.G. Zoebisch, E.F. Healy, J.J.P. Stewart, Development and use of quantum mechanical molecular models. 76. AM1: a new general purpose quantum mechanical molecular model, J. Am. Chem. Soc. 107 (1985) 3902–3909.
[42] M.W. Schmidt, K.K. Baldridge, J.A. Boatz, S.T. Elbert, M.S. Gordon, J.J. Jensen, S. Koseki, N. Matsunaga, K.A. Su, S. Nguyen, T.L. Windus, M. Dupuis, J.A. Montgomery, General atomic and molecular electronic structure system, J. Comput. Chem. 14 (1993) 1347–1363.